Computational statistical mechanics of a confined, three-dimensional Coulomb gas

Sergio Davis [1,2,*] Jalaj Jain [1] and Biswajit Bora [1,2]

[1] *Comisión Chilena de Energía Nuclear, Casilla 188-D, Santiago, Chile*

[2] *Departamento de Física, Facultad de Ciencias Exactas, Universidad Andres Bello, Sazié 2212, Piso 7, 8370136 Santiago, Chile*

(Received 28 April 2020; accepted 8 October 2020; published 28 October 2020)

The thermodynamic properties of systems with long-range interactions present an ongoing challenge, from the point of view of both theory as well as computer simulation. In this paper we study a model system, a Coulomb gas confined inside a sphere, by using the Wang-Landau algorithm. We have computed the configurational density of states, the thermodynamic entropy, and the caloric curve, and compared with microcanonical Metropolis simulations, while showing how concepts such as the configurational inverse temperature can be used to understand some aspects of thermodynamic behavior. A dynamical multistability behavior is seen at low energies in microcanonical Monte Carlo simulations, suggesting that flat-histogram methods can in fact be useful and complementary alternatives to traditional Metropolis simulation in complex systems.

DOI: 10.1103/PhysRevE.102.042137

I. INTRODUCTION

The thermodynamics of charged particles remains a challenging subject, in large part due to the long-range nature of the interaction which breaks some assumptions of classical statistical mechanics, mainly that of additivity of the interaction energy of macroscopic subsystems [1]. While exact results are common for the two-dimensional Coulomb potential [2,3], the situation in three dimensions for the unscreened Coulomb potential is not as clear, even after the use of computer simulation techniques.

One interesting phenomenon in long-range interacting systems is the origin of non-Maxwellian velocity distributions, not only in plasmas but in model systems such as the Hamiltonian mean-field model in nonequilibrium conditions [4,5]. In such long-range systems different mechanisms have been proposed to explain these distributions, such as Tsallis's nonextensive statistical mechanics [6,7], superstatistics [8], and others. For an isolated system, the velocity distribution of its components is governed by properties of the interaction potential, more precisely by its configurational density of states (CDOS), as, for instance, shown by Ray and Graben [9] in small systems. Therefore, it makes sense to gain some understanding of the behavior of this CDOS for long-range potentials.

In the field of condensed matter physics, on the other hand, the computation of the CDOS for systems with complex interactions (such as proteins) using Monte Carlo methods in generalized ensembles has recently emerged as a promising alternative [10,11] to molecular dynamics simulations. Nevertheless, we are not aware of a calculation of the CDOS for pure Coulomb systems in the literature.

In this paper, we focus on the thermodynamics of a very simple model system, where charged particles interacting via the unscreened Coulomb potential are confined inside a spherical region. We present a computation of the CDOS using the Wang-Landau algorithm [12], and from this we determine its equilibrium thermodynamic properties in the canonical and microcanonical ensembles. This spherical geometry is a useful approximation to some relevant configurations of high-density, high-temperature plasmas such as in inertial confinement, where there is interest in modeling the behavior of plasma confined in a small, spherically symmetric regions such that highly energetic ions are able to reach the conditions of temperature and density needed to produce nuclear fusion [13,14].

This paper is organized as follows. Section II defines the interaction energy and the choice of natural units. Sections III and IV review the microcanonical formalism in terms of the configurational degrees of freedom, and the implementation of Monte Carlo methods, while Sec. V presents the main results. Finally we close with some concluding remarks in Sec. VI.

II. DESCRIPTION OF THE MODEL

We will consider a group of $N = N_+ + N_-$ charged particles in three dimensions. The N particles are divided exactly into two equal groups of $N_+ = N_- = N/2$ with charge $q_+ = e$ and $q_- = -e$, respectively, in order to have exact neutrality. In this system, the Hamiltonian is

$$H(\boldsymbol{R}, \boldsymbol{P}) = K(\boldsymbol{P}) + \Phi(\boldsymbol{R}) = \sum_{i=1}^{N} \frac{\boldsymbol{p}_i^2}{2m_i} + \Phi(\boldsymbol{r}_1, \ldots, \boldsymbol{r}_N), \qquad (1)$$

where $\boldsymbol{R} = (\boldsymbol{r}_1, \ldots, \boldsymbol{r}_N)$ and $\boldsymbol{P} = (\boldsymbol{p}_1, \ldots, \boldsymbol{p}_N)$ are the coordinates and momenta of all particles, respectively, $K = K(\boldsymbol{P})$ is the classical (nonrelativistic) kinetic energy,

$$K(\boldsymbol{P}) := \sum_{i=1}^{N} \frac{\boldsymbol{p}_i^2}{2m_i},$$

*sergio.davis@cchen.cl

 ©2020 American Physical Society

TABLE I. Parameters in physical units for the choice of r_0 equal to the Bohr radius.

Description	Symbol	Reference value
Length unit	r_0	0.529 Å
Energy unit	$\phi_0 = e^2/(4\pi\epsilon_0 r_0)$	27.211 eV
Temperature unit	$T_0 = \phi_0/k_B$	315774 K
Number of particles	N	210
Confining radius	R	146 Å
Particle density	$n = N/(\frac{4}{3}\pi R^3)$	8.05×10^{24} m^{-3}
Debye length at $T = T_0$	λ_D	137.1 Å

and $\Phi = \Phi(\boldsymbol{R})$ is the electrostatic potential energy, given by

$$\Phi(\boldsymbol{r}_1, \ldots, \boldsymbol{r}_N) = \frac{1}{2}\sum_{i=1}^{N}\sum_{j\neq i}\frac{q_i q_j}{4\pi\epsilon_0|\boldsymbol{r}_j - \boldsymbol{r}_i|}. \tag{2}$$

The potential energy can be expressed in natural units by defining a natural length unit r_0. We can write

$$\Phi(\boldsymbol{r}_1, \ldots, \boldsymbol{r}_N) = \frac{\phi_0}{2}\sum_{i=1}^{N}\sum_{j\neq i}\frac{\sigma_i\sigma_j}{r_{ij}}, \tag{3}$$

with $\sigma_i = \pm 1$ and the distance between particles i and j being $r_{ij} := |\boldsymbol{r}_j - \boldsymbol{r}_i|$ in units of r_0. With these changes, the model now resembles a long-range Ising-type interaction but with mobile "spins." The unit of energy corresponds to

$$\phi_0 := \frac{e^2}{4\pi\epsilon_0 r_0}. \tag{4}$$

At this point, we will introduce two modifications to the model. First, in order to "soften" the interaction at very short distances, we have corrected the interparticle distance r_{ij} as

$$r_{ij} \to \max(r_{ij}, r_0),$$

which avoids the singular behavior at $r_{ij} = 0$, making the potential energy bounded. As shown originally by Fisher and Ruelle [15], this truncation of the Coulomb potential is one mechanism able to restore stability. Second, because our aim is to describe an isolated, finite-size system, the particles are confined inside a sphere of radius R, so that $|\boldsymbol{r}_i| < R$.

In the following we use $N = 210$ particles and a confining radius $R = 276\ r_0$. We have chosen this number of particles as a practical tradeoff between computational efficiency and detail of the description, considering that larger systems can be described by thinking in terms of a coarse graining using so-called superparticles, in which one particle represents a larger unit of charge and mass.

For reference, the values of some parameters of interest in plasma physics are given in Table I, for the choice of r_0 equal to the Bohr radius, $r_0 = 0.529$ Å. In this case, the system is denser than magnetic confinement plasmas but less dense than inertial fusion plasmas [16]. Because the Debye length $\lambda_D \sim 0.94R$ is of the order of the radius of the confining sphere, most of the system is contained within the Debye sphere and we do not expect much screening of the charges.

III. MICROCANONICAL THERMODYNAMICS

For a system with a Hamiltonian given by Eq. (1), because the form of the kinetic energy is universal, the CDOS becomes the key quantity for the thermodynamics in steady states. We will consider a steady state S described by the ensemble function $\rho(E)$, such that

$$P(\boldsymbol{R}, \boldsymbol{P}|S) = \rho[H(\boldsymbol{R}, \boldsymbol{P})]. \tag{5}$$

In such an ensemble, the expectation of any function $g(H)$ of the energy can be computed as

$$\begin{aligned}\langle g\rangle_S &= \int d\boldsymbol{R}d\boldsymbol{P}\ g[H(\boldsymbol{R}, \boldsymbol{P})]\ P(\boldsymbol{R}, \boldsymbol{P}|S)\\ &= \int d\boldsymbol{R}d\boldsymbol{P}\ g[K(\boldsymbol{P}) + \Phi(\boldsymbol{R})]\rho[K(\boldsymbol{P}) + \Phi(\boldsymbol{R})].\end{aligned} \tag{6}$$

Let us at this point introduce the density of states $\Omega_K(k)$ of the classical ideal gas:

$$\Omega_K(k) := \int d\boldsymbol{P}\ \delta[K(\boldsymbol{P}) - k], \tag{7}$$

with δ the Dirac delta function, and the configurational density of states $\mathcal{D}(\phi)$, defined in our case by the multidimensional integral

$$\begin{aligned}\mathcal{D}(\phi) &:= \int d\boldsymbol{R}\delta[\phi - \Phi(\boldsymbol{R})]\\ &= \int_{\mathcal{S}(R)} d\boldsymbol{r}_1, \ldots, d\boldsymbol{r}_N\ \delta[\phi - \Phi(\boldsymbol{r}_1, \ldots, \boldsymbol{r}_N)],\end{aligned} \tag{8}$$

where $\int_{\mathcal{S}(R)}$ denotes integration over the region $|\boldsymbol{r}_i| < R$ for $i = 1, \ldots, N$. Using these densities of states, we can rewrite the $6N$-dimensional integral in Eq. (6) as a two-dimensional integral:

$$\begin{aligned}\langle g\rangle_S &= \int d\boldsymbol{R}d\boldsymbol{P}\ g[K(\boldsymbol{P}) + \Phi(\boldsymbol{R})]\rho[K(\boldsymbol{P}) + \Phi(\boldsymbol{R})]\\ &= \int d\boldsymbol{R}\int dk\left\{\int d\boldsymbol{P}\delta[k - K(\boldsymbol{P})]\right\}g[k + \Phi(\boldsymbol{R})]\rho[k + \Phi(\boldsymbol{R})]\\ &= \int dk\ \Omega_K(k)\int d\phi\left\{\int d\boldsymbol{R}\delta[\phi - \Phi(\boldsymbol{R})]\right\}g(k + \phi)\rho(k + \phi)\\ &= \int dk\ d\phi\ \Omega_K(k)\mathcal{D}(\phi)g(k + \phi)\rho(k + \phi),\end{aligned} \tag{9}$$

where k and ϕ are integration variables that go through all allowed values of $K(\boldsymbol{P})$ and $\Phi(\boldsymbol{R})$, respectively.

The density of states of the classical ideal gas can be computed exactly as

$$\Omega_K(k) = \int d\boldsymbol{p}_1 \dots d\boldsymbol{p}_N \, \delta\left(\sum_{i=1}^{N} \frac{\boldsymbol{p}_i^2}{2m_i} - k\right) = \Omega_0 \, k^{\frac{3N}{2}-1}, \tag{10}$$

where $\Omega_0 = \Omega_0(N, V)$ is a constant the exact value of which plays no role in the statistical properties at constant volume and number of particles. It is given by

$$\Omega_0 = \left(\frac{V}{h^3}\right)^N \frac{(2\pi)^{3N/2}}{\Gamma\left(\frac{3N}{2}\right)} \prod_{i=1}^{N} (m_i)^{3/2},$$

where h is Planck's constant [17]. In the following we will focus on the microcanonical ensemble, representing a system with fixed energy $H = E$, and given by

$$P(\boldsymbol{R}, \boldsymbol{P}|E) = \frac{\delta[E - H(\boldsymbol{R}, \boldsymbol{P})]}{\Omega(E)}, \tag{11}$$

with $\Omega(E)$ the density of states, defined as

$$\begin{aligned}\Omega(E) &:= \int d\boldsymbol{R} d\boldsymbol{P} \delta[E - H(\boldsymbol{R}, \boldsymbol{P})] \\ &= \Omega_0 \int d\boldsymbol{R} \int dk \; \delta[E - k - \Phi(\boldsymbol{R})] k^{\frac{3N}{2}-1} \\ &= \Omega_0 \int d\boldsymbol{R} [E - \Phi(\boldsymbol{R})]_+^{\frac{3N}{2}-1},\end{aligned} \tag{12}$$

and where expectations are computed by

$$\langle g \rangle_E = \frac{1}{\Omega(E)} \int d\boldsymbol{R} d\boldsymbol{P} \delta[E - H(\boldsymbol{R}, \boldsymbol{P})] g(\boldsymbol{R}, \boldsymbol{P}). \tag{13}$$

This ensemble is important for at least two reasons. On the one hand, the microcanonical ensemble is the appropriate description for an isolated system with constant volume and number of particles, but it also can be taken as the basis for the thermodynamics of any generalized ensemble. In fact, the expectation on any generalized ensemble S of the form in Eq. (5) is given by Eq. (6), which can be written as

$$\begin{aligned}\langle g \rangle_S &= \int d\boldsymbol{R} d\boldsymbol{P} P(\boldsymbol{R}, \boldsymbol{P}|S) \cdot g(\boldsymbol{R}, \boldsymbol{P}) \\ &= \int d\boldsymbol{R} d\boldsymbol{P} \rho[H(\boldsymbol{R}, \boldsymbol{P})] \cdot g(\boldsymbol{R}, \boldsymbol{P}) \\ &= \int dE \left\{ \int d\boldsymbol{R} d\boldsymbol{P} \delta[E - H(\boldsymbol{R}, \boldsymbol{P})] g(\boldsymbol{R}, \boldsymbol{P}) \right\} \rho(E) \\ &= \int dE \, \rho(E) \times \{\Omega(E) \langle g \rangle_E\} \\ &= \int dE P(E|S) \langle g \rangle_E,\end{aligned} \tag{14}$$

that is, generalized ensemble expectations can be computed from microcanonical expectations and the distribution of energy of the ensemble:

$$P(E|S) = \rho(E)\Omega(E).$$

The microcanonical configurational distribution is obtained by integration of Eq. (11) over the momenta:

$$\begin{aligned}P(\boldsymbol{R}|E) &= \int d\boldsymbol{P} P(\boldsymbol{R}, \boldsymbol{P}|E) \\ &= \int d\boldsymbol{P} \left[\frac{\delta[E - K(\boldsymbol{P}) - \Phi(\boldsymbol{R})]}{\Omega(E)} \right] \\ &= \int dK \Omega_K(K) \frac{\delta[E - K - \Phi(\boldsymbol{R})]}{\Omega(E)} \\ &= \frac{\Omega_K[E - \Phi(\boldsymbol{R})]}{\Omega(E)}.\end{aligned} \tag{15}$$

Replacing the definition of Ω_K in Eq. (10) we have

$$P(\boldsymbol{R}|E) = \frac{1}{\eta(E)} [E - \Phi(\boldsymbol{R})]_+^{\frac{3N}{2}-1}, \tag{16}$$

where $[x]_+ = x$ for $x >= 0$ and zero otherwise. The normalization constant $\eta(E)$ is given by

$$\eta(E) = \int d\boldsymbol{R} [E - \Phi(\boldsymbol{R})]_+^{\frac{3N}{2}-1} = \frac{\Omega(E)}{\Omega_0}. \tag{17}$$

Using the CDOS it is possible to write the microcanonical probability density of ϕ as

$$P(\phi|E) = \langle \delta(\phi - \Phi) \rangle_E = \frac{1}{\eta(E)} [E - \phi]_+^{\frac{3N}{2}-1} \mathcal{D}(\phi). \tag{18}$$

The entropy $S(E)$ can also be expressed [18] in terms of $\eta(E)$ in Eq. (17):

$$S(E) = k_B \ln \Omega_0 + k_B \ln \eta(E). \tag{19}$$

By differentiation with respect to E, it follows that the microcanonical inverse temperature $\beta(E)$, defined as

$$\beta(E) := \frac{1}{k_B T(E)} = \frac{1}{k_B} \frac{\partial S(E)}{\partial E} = \frac{\partial}{\partial E} \ln \eta(E), \tag{20}$$

can be computed as

$$\begin{aligned}\frac{\partial}{\partial E} \ln \eta(E) &= \frac{1}{\eta(E)} \frac{\partial}{\partial E} \left(\int d\phi \mathcal{D}(\phi) [E - \phi]_+^{\frac{3N}{2}-1} \right) \\ &= \frac{1}{\eta(E)} \int d\phi \mathcal{D}(\phi) \frac{\partial}{\partial E} \left([E - \phi]_+^{\frac{3N}{2}-1} \right) \\ &= \frac{1}{\eta(E)} \int d\phi \mathcal{D}(\phi) [E - \phi]_+^{\frac{3N}{2}-1} \left(\frac{3N - 2}{2(E - \phi)} \right) \\ &= \left\langle \frac{3N - 2}{2(E - \phi)} \right\rangle_E,\end{aligned} \tag{21}$$

which gives us the kinetic estimator of the inverse temperature:

$$\beta_K(\phi) := \frac{3N - 2}{2(E - \phi)}, \tag{22}$$

such that $\langle \beta_K \rangle_E = \beta(E)$. In a similar way as the microcanonical inverse temperature $\beta(E)$ is defined in terms of the full density of states [either $\Omega(E)$ or $\eta(E)$], it is possible to define an inverse temperature from the CDOS, namely, the *configurational inverse temperature*, as

$$\beta_{\mathcal{D}}(\phi) := \frac{\partial}{\partial \phi} \ln \mathcal{D}(\phi), \tag{23}$$

for which it holds that $\langle\beta_{\mathcal{D}}\rangle_E = \langle\beta_K\rangle_E = \beta(E)$. This can be seen from the conjugate variables theorem [19,20] applied to the potential energy distribution in Eq. (18):

$$\left\langle \frac{\partial\omega}{\partial\phi} \right\rangle_E = -\left\langle \omega(\phi)\frac{\partial}{\partial\phi}\ln P(\phi|E) \right\rangle_E = \langle\omega(\phi)[\beta_K(\phi) - \beta_{\mathcal{D}}(\phi)]\rangle_E, \tag{24}$$

for $\omega = \omega(\phi)$ an arbitrary, differentiable function of ϕ. For the choice $\omega(\phi) = 1$, we have

$$\langle\beta_K\rangle_E = \langle\beta_{\mathcal{D}}\rangle_E. \tag{25}$$

IV. COMPUTATIONAL METHODS

For the calculation of the density of states, in this case $\mathcal{D}(\phi)$, several methods exist. One of the most widely known is the Wang-Landau procedure [12], in which a Markov process is performed in configuration space according to the transition probability

$$p_{\rm acc}(\boldsymbol{R} \to \boldsymbol{R}') = \min\left(1, \frac{\mathcal{D}[\Phi(\boldsymbol{R})]}{\mathcal{D}[\Phi(\boldsymbol{R}')]}\right),$$

which is the probability of accepting a "move" from configuration $\boldsymbol{R}$ to $\boldsymbol{R}'$. This process achieves a flat distribution of potential energies as the Markov chain dynamics converges to the generalized ensemble:

$$\rho(\phi) \propto 1/\mathcal{D}(\phi).$$

Because the value of $\mathcal{D}(\phi)$ is not known *a priori*, the procedure starts with an initial guess (usually uniform) and updates it for every visited potential energy ϕ_i using the rule

$$\mathcal{D}(\phi_i) \to \mathcal{D}(\phi_i) f.$$

In the traditional Wang-Landau algorithm, as implemented in this paper, the factor f is decreased from an initial value $f = e = 2.718\,28...$following the rule $f_{i+1} = \sqrt{f_i}$ so that it converges to 1.

Microcanonical simulations at constant total energy E, in the ensemble defined by Eq. (16), can be performed via Monte Carlo Metropolis as proposed by Ray [21], in which the acceptance probability becomes

$$p_{\rm acc}(\boldsymbol{R} \to \boldsymbol{R}') = \min\left(1, \left[\frac{E - \Phi(\boldsymbol{R}')}{E - \Phi(\boldsymbol{R})}\right]^{\frac{3N}{2}-1}\right), \tag{26}$$

instead of the usual

$$p_{\rm acc}(\boldsymbol{R} \to \boldsymbol{R}') = \min(1, \exp(-\beta\Delta\phi)), \tag{27}$$

employed in canonical Metropolis simulation. Note that, for $|\Delta\phi| \ll E - \Phi$ where $\Delta\phi = \Phi(\boldsymbol{R}') - \Phi(\boldsymbol{R})$, we can provide the following convenient approximation:

$$\begin{aligned}\left[\frac{E - \Phi(\boldsymbol{R}')}{E - \Phi(\boldsymbol{R})}\right]^{\frac{3N}{2}-1} &= \left[\frac{E - \Phi(\boldsymbol{R}) - \Delta\phi}{E - \Phi(\boldsymbol{R})}\right]^{\frac{3N}{2}-1} \\ &= \left[1 - \frac{\Delta\phi}{E - \Phi(\boldsymbol{R})}\right]^{\frac{3N}{2}-1} \\ &= \exp\left[\frac{3N-2}{2}\ln\left(1 - \frac{\Delta\phi}{E - \Phi(\boldsymbol{R})}\right)\right] \\ &\approx \exp\{-\beta_K[\Phi(\boldsymbol{R})]\Delta\phi\}. \end{aligned} \tag{28}$$

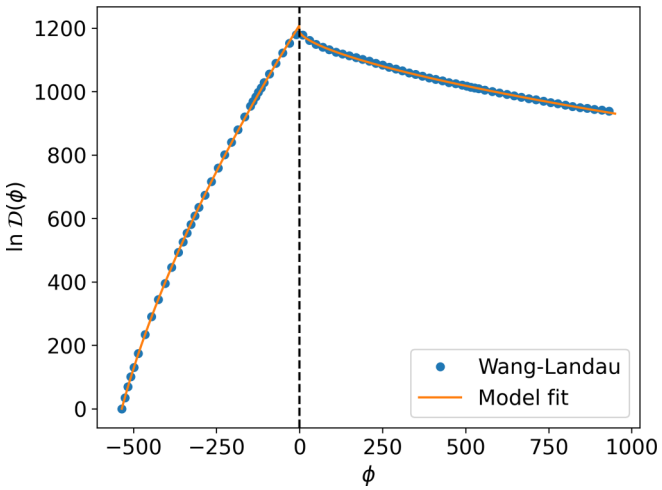

FIG. 1. Logarithm of the configurational density of states $\mathcal{D}(\phi)$ for a Coulomb system confined to a sphere, for energies Φ between $-535\ \phi_0$ and $950\ \phi_0$, as computed by the Wang-Landau algorithm (blue circles) and fitted by Eq. (29) (orange solid line). The black dashed line indicates $\phi = 0$, the value above which the curvature changes.

This means that, for small proposed displacements, microcanonical Metropolis sampling can be treated as a canonical Metropolis sampling with variable inverse temperature, given by β_K in Eq. (22). In the case of vanishing potential energy fluctuations, the microcanonical ensemble predictions coincide with the canonical predictions at $\beta = \beta(E)$.

V. RESULTS

For the system of N particles interacting via Φ in Eq. (3) inside a sphere of radius R, the logarithm of the CDOS calculated using the Wang-Landau algorithm is shown in Fig. 1. Wang-Landau simulations were performed independently on eight overlapping subintervals of energy (with an overlap of at least ten units of energy) and the CDOS was joined together based on the matching of the overlapping regions. For each subinterval, the Wang-Landau simulation reached a factor $f - 1 = 10^{-10}$ or smaller, and accordingly the error bars for the logarithm of the CDOS are much smaller than the circles in Fig. 1.

It can be seen that the CDOS is asymmetrical, having a cusp exactly at $\phi = 0$ at which the derivatives are different left and right. These left and right regions can be described by the simple empirical model

$$\ln\mathcal{D}(\phi) = \begin{cases} a + A(\phi + b)^{\alpha}, & \text{if } \phi < 0, \\ a + Ab^{\alpha} - B\phi^{\alpha}, & \text{if } \phi \geqslant 0, \end{cases} \tag{29}$$

with parameters $a = -596.0357$, $b = 626.8341$, $A = 44.9553$, $B = 5.3482$, and $\alpha = 0.5731$.

Regarding the size dependence of the density of states, if we consider the ansatz where the configurational inverse temperature, being an intensive quantity, only depends on the potential energy per particle in the thermodynamic limit, we can write

$$\lim_{N\to\infty} \beta_{\mathcal{D}}(\phi) = g(\phi/N) \tag{30}$$

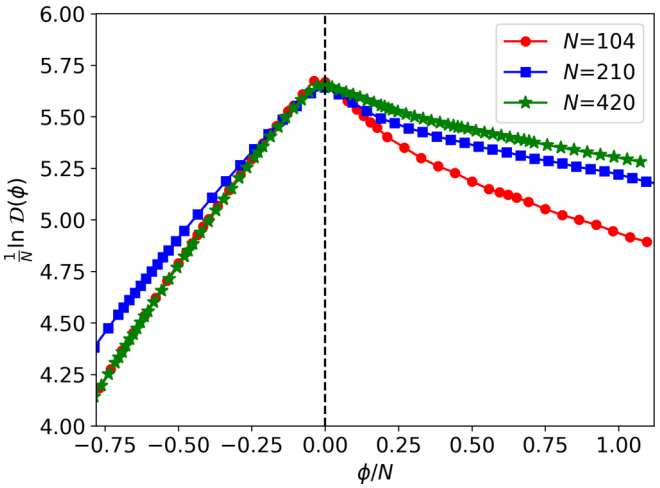

FIG. 2. Rescaled logarithm of the configurational density of states for different system sizes at the same particle density: $N = 104$ (red circles), $N = 210$ (blue squares), and $N = 420$ (green stars).

where g is an appropriate function describing the system. Then, it would follow by integration in ϕ that

$$\lim_{N\to\infty} \ln \mathcal{D}(\phi) = \int d\phi\, g(\phi/N) = NG(\phi/N) + \zeta(N). \quad (31)$$

This dependence on the system size is shown in Fig. 2, where we plot $\frac{1}{N}\ln \mathcal{D}(\phi)$ as a function of ϕ/N for three different sizes, $N = 104$, 210, and 420. We see that the general dependence in Eq. (31) seems to hold approximately.

The configurational inverse temperature β_D, defined in Eq. (23), is shown in Fig. 3. A discontinuity at $\phi = 0$ can be seen, reflecting the change in curvature of the CDOS. Because $\beta_D < 0$ for $\phi > 0$, an interesting fact arises, namely, that no macroscopic state S is compatible with strictly positive potential energies. For instance, in the microcanonical ensemble at energy E this would imply

$$\langle \beta_D \rangle_E = \langle \beta_K \rangle_E < 0, \quad (32)$$

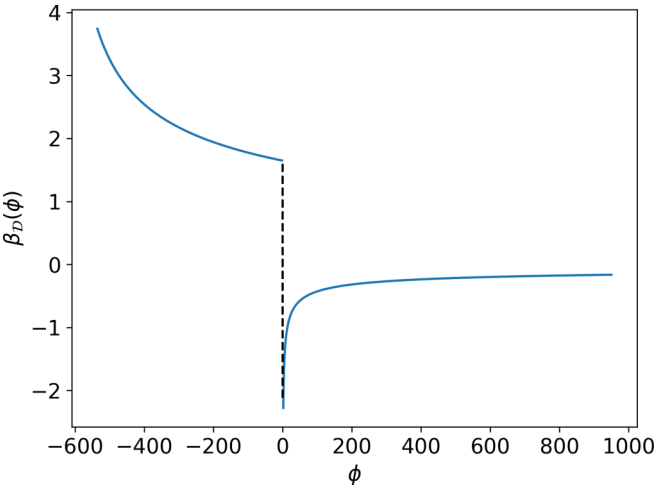

FIG. 3. Configurational inverse temperature $\beta_{\mathcal{D}}(\phi)$ (blue solid line) obtained from the CDOS in Fig. 1. The black dashed line indicates the discontinuity at $\phi = 0$.

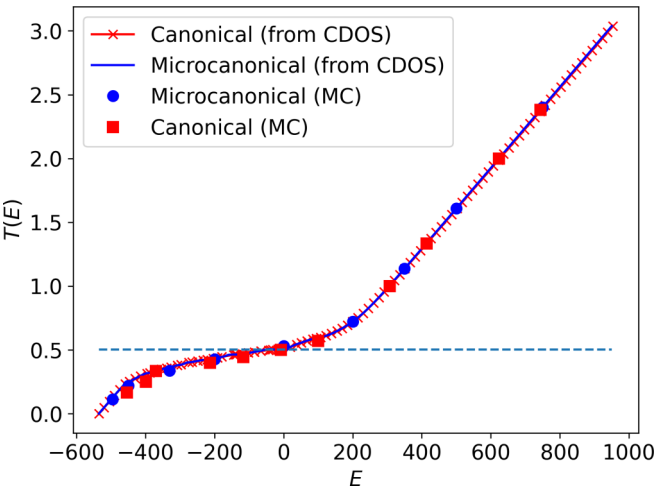

FIG. 4. Caloric curve $T(E)$ for a Coulomb system confined to a sphere, for energies E between $-535\ \phi_0$ and $950\ \phi_0$ units. Blue circles represent microcanonical Metropolis simulations, while red squares indicate canonical Metropolis simulations. The solid blue line and the red line with crosses are the microcanonical and canonical predictions, respectively, based on the CDOS in Fig. 1. The horizontal dashed line corresponds to the temperature $T = 0.5\,T_0$ at $E = 0$.

which contradicts the definition of

$$\beta_K(\phi) = \frac{3N}{2(E-\phi)} > 0.$$

A consequence of this contradiction is the fact that the potential energies tend to "pile up" towards $\phi = 0$ for high enough total energies, as can be seen in the lower panel of Fig. 6 for energies up to $E = 3000\,\phi_0$. In other words, despite the fact that microscopic states with ϕ even above $900\ \phi_0$ do exist, as shown by the CDOS in Fig. 1, they are in practice suppressed in the microcanonical ensemble and in any generalized ensemble. By using Eqs. (14) and (25), we see that in general

$$\langle \beta_K \rangle_S = \int dE P(E|S) \langle \beta_K \rangle_E = \int dE P(E|S) \langle \beta_{\mathcal{D}} \rangle_E = \langle \beta_{\mathcal{D}} \rangle_S, \quad (33)$$

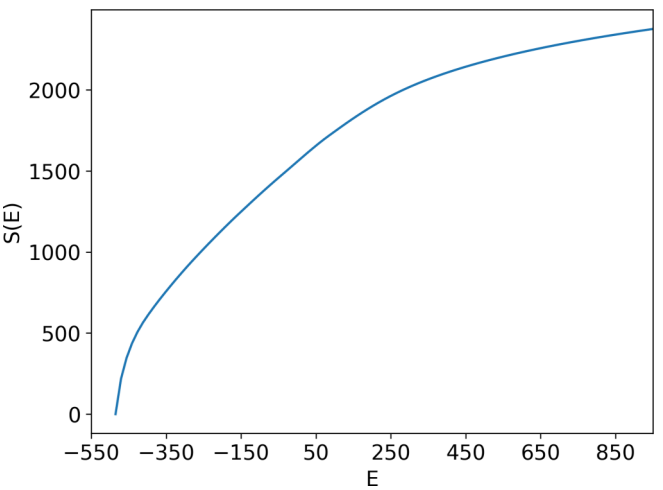

FIG. 5. Total entropy for a Coulomb system confined to a sphere, for energies E between $-535\ \phi_0$ and $950\ \phi_0$.

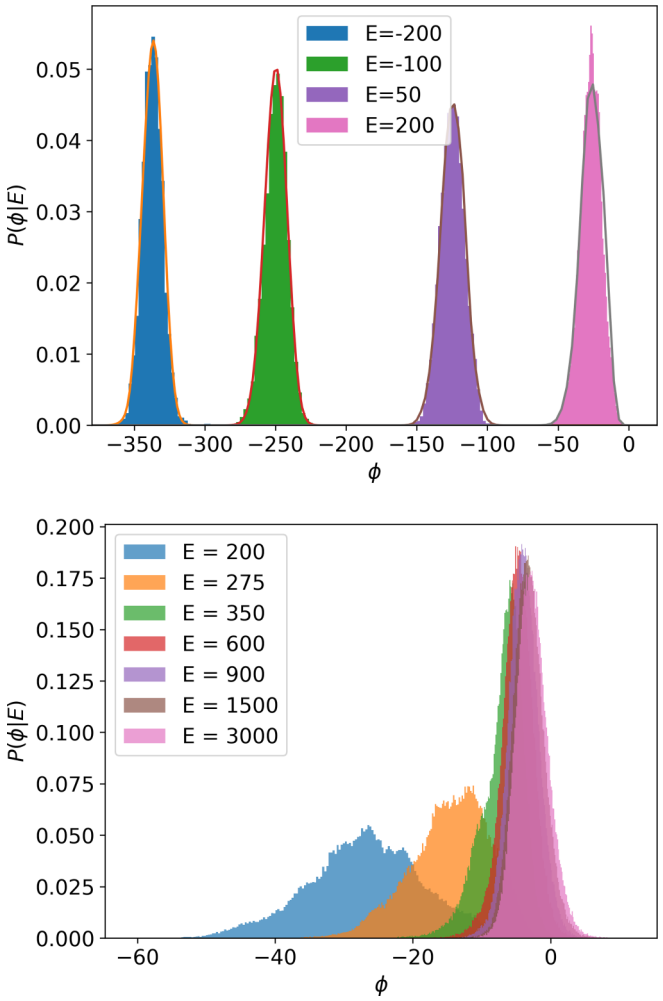

FIG. 6. Upper panel: Potential energy histograms from microcanonical Monte Carlo simulation, from left to right going from $E = -200\,\phi_0$ to $200\,\phi_0$. The solid lines are the corresponding probability densities predicted using Eq. (18). Lower panel: Potential energy histograms for microcanonical simulation for total energies (from left to right) between $E = 200\,\phi_0$ and $3000\,\phi_0$, showing the concentration of the distribution mass towards $\phi = 0$.

so $P(\phi < 0|S) \to 0$ would imply $\langle \beta_{\mathcal{D}} \rangle_S < 0$ and therefore $\langle \beta_K \rangle_S < 0$, which goes against the positivity of kinetic energy.

Thermodynamical properties

Using the microcanonical Monte Carlo method defined by the acceptance probability in Eq. (26), we have computed the caloric curve $T(E)$ by collecting the average

$$\beta(E) = \frac{1}{k_B T(E)} = \left\langle \frac{3N-2}{2(E-\Phi)} \right\rangle_E ,$$

and compared with the predictions of Eqs. (21) and (18) with the CDOS in Fig. 1. This caloric curve is shown in Fig. 4, together with independent canonical Monte Carlo simulations, using the acceptance probability in Eq. (27) instead.

Complete equivalence between both ensembles is seen, despite the fact that a transition seems to occur between two branches with nearly constant specific heat, around

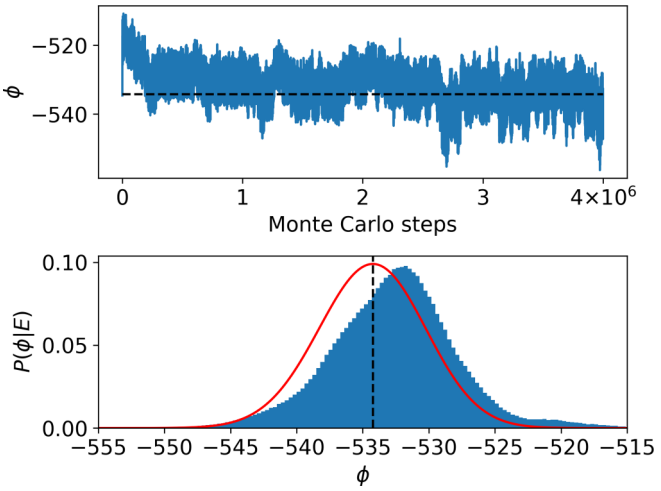

FIG. 7. Upper panel: Potential energy as a function of Monte Carlo steps in the microcanonical ensemble, for $E = -450\,\phi_0$. Lower panel: Histogram of the potential energy collected in the same simulation. The dashed black line indicates the most probable potential energy, given by Eq. (34). Due to the dynamic multistability phenomenon observed, the convergence of the histogram to the correct distribution (red solid line) given by Eq. (18) is much slower than for other energies.

$T^* = 0.5\,T_0$, the temperature corresponding to $E = 0$. The continuous behavior of the caloric curve is verified in the microcanonical entropy $S(E) = k_B \ln \eta(E)$, shown in Fig. 5. The entropy is monotonically increasing with E without any "backbending," thus despite the discontinuity of the configurational inverse temperature there is no evidence in this system of a first-order phase transition, as is sometimes the case in long-range interacting [1] and small systems [22].

In order to assess the accuracy of the CDOS computed using the Wang-Landau algorithm beyond averages, we computed the microcanonical potential energy distributions according to Eq. (18) for several total energies, and compared them with empirical histograms collected from microcanonical Monte Carlo simulation. These results are shown in Fig. 6. We can see that, in all cases, the CDOS is capable of describing correctly the shape of the potential energy fluctuations, at least above $E = -200\,\phi_0$. In the lower branch of the caloric curve, however, an interesting phenomenon of dynamical multistability is observed in the microcanonical Monte Carlo simulation, as shown for $E = -450\,\phi_0$ in Fig. 7. In this case, even when the simulation starts from the most probable potential energy, given by the condition

$$\frac{\partial}{\partial \phi} \ln P(\phi|E)\Big|_{\phi=\phi^*} = 0,$$

that is,

$$\beta_K(\phi^*) = \beta_{\mathcal{D}}(\phi^*), \tag{34}$$

which has solution $\phi^* = -534.231\ \phi_0$ for $E = -450\,\phi_0$ (shown as the black dashed line in Fig. 7), the system transits between several macroscopic states, with considerable lifetimes. This effect resembles the behavior of glasses [23] and proteins [24], which commonly have a complex potential energy landscape that makes direct sampling difficult. The

dynamical multistability phenomenon reduces the efficiency of microcanonical sampling for low energies, as we have to wait much longer times for the system to explore the different macroscopic states with the correct frequency, thus requiring extremely long simulations to collect reliable statistics.

VI. CONCLUDING REMARKS

We have computed thermodynamic properties of a system of unscreened charged particles confined into a spherical region by using one of the well-established flat-histogram methods, the Wang-Landau algorithm. Our system, while conceptually simple, is still challenging from the point of view of computational statistical mechanics, as we have shown in direct microcanonical Metropolis sampling. We have determined the thermodynamics of the system; in particular, we report the configurational density of states, the full thermodynamic entropy, the caloric curve, and the microcanonical potential energy distributions. We observe a possibly second-order phase transition at $E = 0$, the precise nature and order of which remain to be clarified by further analysis.

The shape of the configurational inverse temperature easily explains a concentration of the potential energy distribution mass around $\Phi = 0$ at high total energies, which makes most states with $\Phi > 0$ inaccessible from the microcanonical ensemble. On the other hand, the presence of a dynamical multistability phenomenon complicates the direct microcanonical sampling at low energies, highlighting the usefulness of the generalized-ensemble approaches to computational statistical mechanics.

ACKNOWLEDGMENT

The authors gratefully acknowledge funding from Anillo Grant No. ACT-172101.

[1] A. Campa, T. Dauxois, and S. Ruffo, Statistical mechanics and dynamics of solvable models with long-range interactions, Phys. Rep. **480**, 57 (2009).

[2] V. M. Bedanov and F. M. Peeters, Ordering and phase transitions of charged particles in a classical finite two-dimensional system, Phys. Rev. B **49**, 2667 (1994).

[3] L. Samaj, The statistical mechanics of the classical two-dimensional Coulomb gas is exactly solved, J. Phys. A: Math. Gen. **36**, 5913 (2003).

[4] V. Latora, A. Rapisarda, and C. Tsallis, Fingerprints of nonextensive thermodynamics in a long-range Hamiltonian system, Physica A **305**, 129 (2002).

[5] B. Atenas and S. Curilef, Dynamics and thermodynamics of systems with long-range dipole-type interactions, Phys. Rev. E **95**, 022110 (2017).

[6] J. L. Du, Nonextensivity in nonequilibrium plasma systems with Coulombian long-range interactions, Phys. Lett. A **329**, 262 (2004).

[7] C. Tsallis, A. Rapisarda, A. Pluchino, and E. P. Borges, On the non-Boltzmannian nature of quasi-stationary states in long-range interacting systems, Phys. A **381**, 143 (2007).

[8] C. Beck, Superstatistics: Theory and applications, Continuum Mech. Thermodyn. **16**, 293 (2004).

[9] J. R. Ray and H. W. Graben, Small systems have non-Maxwellian momentum distributions in the microcanonical ensemble, Phys. Rev. A **44**, 6905 (1991).

[10] N. Rathore, T. A. Knotts, IV, and J. J. de Pablo, Configurational temperature density of states simulations of proteins, Biophys. J. **85**, 3963 (2003).

[11] N. Rathore, T. A. Knotts, and J. J. de Pablo, Density of states simulations of proteins, J. Chem. Phys. **118**, 4285 (2003).

[12] F. Wang and D. P. Landau, Efficient, Multiple-Range Random Walk Algorithm to Calculate the Density of States, Phys. Rev. Lett. **86**, 2050 (2001).

[13] H. Matsuura, T. Takaki, K. Funakoshi, Y. Nakao, and K. Kudo, Ion distribution function and radial profile of neutron production rate in spherical inertial electrostatic confinement plasmas, Nucl. Fusion **40**, 1951 (2000).

[14] B. E. Peigney, O. Larroche, and V. Tikhonchuk, Fokker–planck kinetic modeling of suprathermal α-particles in a fusion plasma, J. Comput. Phys. **278**, 416 (2014).

[15] M. E. Fisher and D. Ruelle, The stability of many-particle systems, J. Math. Phys. **7**, 260 (1966).

[16] P. M. Bellan, *Fundamentals of Plasma Physics* (Cambridge University Press, Cambridge, England, 2006).

[17] W. Greiner, L. Neise, and H. Stöcker, *Thermodynamics and Statistical Mechanics* (Springer, New York, 2012).

[18] S. Davis, Calculation of microcanonical entropy differences from configurational averages, Phys. Rev. E **84**, 050101(R) (2011).

[19] S. Davis and G. Gutiérrez, Conjugate variables in continuous maximum-entropy inference, Phys. Rev. E **86**, 051136 (2012).

[20] S. Davis and G. Gutiérrez, Applications of the divergence theorem in Bayesian inference and MaxEnt, AIP Conf. Proc. **1757**, 20002 (2016).

[21] J. R. Ray, Microcanonical ensemble Monte Carlo method, Phys. Rev. A **44**, 4061 (1991).

[22] M. Eryürek and M. H. Güven, Negative heat capacity of Ar55 cluster, Physica A **377**, 514 (2007).

[23] J. Ghosh, B. Y. Wong, Q. Sun, F. R. Pon, and R. Faller, Simulations of glasses: Multiscale modeling and density of states Monte-Carlo simulations, Mol. Simul. **32**, 175 (2006).

[24] T. Wüst, Y. W. Li, and D. P. Landau, Unraveling the beautiful complexity of simple lattice model polymers and proteins using Wang-Landau sampling, J. Stat. Phys. **144**, 638 (2011).